Heliyon

Received:
1 August 2018
Revised:
11 December 2018
Accepted:
14 January 2019

Cite as: Bokanda Ekoko Eric, Ekomane Emile, Kenfack Nguemo Gatien Romuald, Njilah Konfor Isaac, Ashukem Nkongho Ethel, Tematio Paul, Bisse Salomon Betrant, Ngueutchoua Gabriel, Orock Ngui Shelly, Belinga Belinga Cedric. Provenance, paleoclimate and diagenetic signatures of sandstones in the Mamfe Basin (West Africa). Heliyon 5 (2019) e01140. doi: 10.1016/j.heliyon.2019.e01140

Provenance, paleoclimate and diagenetic signatures of sandstones in the Mamfe Basin (West Africa)

Bokanda Ekoko Eric [a,*], **Ekomane Emile** [a], **Kenfack Nguemo Gatien Romuald** [b], **Njilah Konfor Isaac** [a], **Ashukem Nkongho Ethel** [a], **Tematio Paul** [b], **Bisse Salomon Betrant** [a], **Ngueutchoua Gabriel** [a], **Orock Ngui Shelly** [a], **Belinga Belinga Cedric** [a]

[a] *University of Yaoundé I, Cameroon*

[b] *University of Dschang, Cameroon*

[*] Corresponding author.

E-mail address: eric_ekoko@yahoo.com (B.E. Eric).

Abstract

Petrography, heavy mineral and trace element geochemistry have been used to unravel the tectonic setting, source area lithology, diagenesis and paleoclimate conditions of the Mamfe sandstones. Quartz exists as monocrystalline (79%), and polycrystalline grains (21%). Orthoclase and microcline are the most dominant feldspars in the rocks. Heavy minerals such as zircon, tourmaline, kyanite, augite, garnets, hornblende, epidotes, diopside, muscovites, biotites, and opaque minerals were disclosed by the samples after bromoform separation. These sandstones are mineralogically and texturally immature and have been classified as arkose on the basis of the QFR diagram. QtFL plot indicates derivation mainly from a transitional continental region of continental block provenance with trace elements geochemical data pointing to a felsic source. The felsic sources are related to the Precambrian granitic/gneissic rocks which formed the basement and margins of the basin. The bivariant log-log Qt/F+R and Qp/F+R plot and the nature of quartz grains of the studied sandstone specimens indicate a semi-humid climatic condition prevailed at the time of deposition in a fluvial

https://doi.org/10.1016/j.heliyon.2019.e01140

environment. The sandstones display deformation of mica, cementation, replacement, and albitization with some having an imprinted reddish brown color indicating a redoxmorphic, locomorphic and phyllomorphic diagenetic stages associated to early, burial and uplift diagenetic processes.

Keywords: Earth sciences, Geology, Geoscience

1. Introduction

Sandstone detrital modes are used to detect information on provenance, palaeoclimate, transport mechanisms, depositional environment and diagenetic characteristics (Dickinson, 1988; Boggs, 2006; Critelli, 2018). According to Christopher et al. (2017) petrography of sandstones discloses clasts composition to major minerals components like quartz, feldspars, rock fragments, accessory mineral, heavy minerals and binding elements (matrix or cement). Quartz mineral distinction, the composition of feldspars and rock fragment reveals sandstone classification and litho-tectonic provenance settings. According to Basu et al. (1975), quartz-grain varieties enclosed in sandstones is indicative of parent-rock assemblages. Heavy mineral petrography provides evidence to source rock composition, as it discloses minerals which carry directly the signatures of the parent rocks (Srivastava et al., 2015; Christopher et al., 2017; Ahmer and Muhammad, 2017). The scope of this work is to identify (1) the source area provenance, (2) palaeoclimate and (3) diagenetic stages of the sandstones in the Mamfe Basin.

2. Geological setting

The Mamfe basin has been described as a rift splay, which is genetically linked with the Benue Trough (Eyong et al., 2013). This basin is found in the south west region of Cameroon which falls within the western part of Africa (Fig. 1). The Basin is also thought to have been formed during Albian to Cenomanian as a result of basement rifting associated with the reactivation of E-W trending mylonite zones within the Panafrican basement. The rift propagated along existing lines of weakness and broadened during the Upper Jurassic time (Kanouo et al., 2015). Rifting in the Mamfe Basin discontinued in the upper Albian to the Lower Cenomanian, due to the sub-crustal contraction that leads the westward displacement of it depositional axis (Kanouo et al., 2012). Rifting in this basin is believed to have been accompanied by rapid subsidence due to the thermal recovery of the lithosphere following a thermal disturbance that leads to stretching and thinning of the crust beneath the basin (Eyong et al., 2013). Its formation is associated with the breaking up of Gondwanaland and subsequent separation of South America plate from Africa plate (Eyong et al., 2013).

https://doi.org/10.1016/j.heliyon.2019.e01140

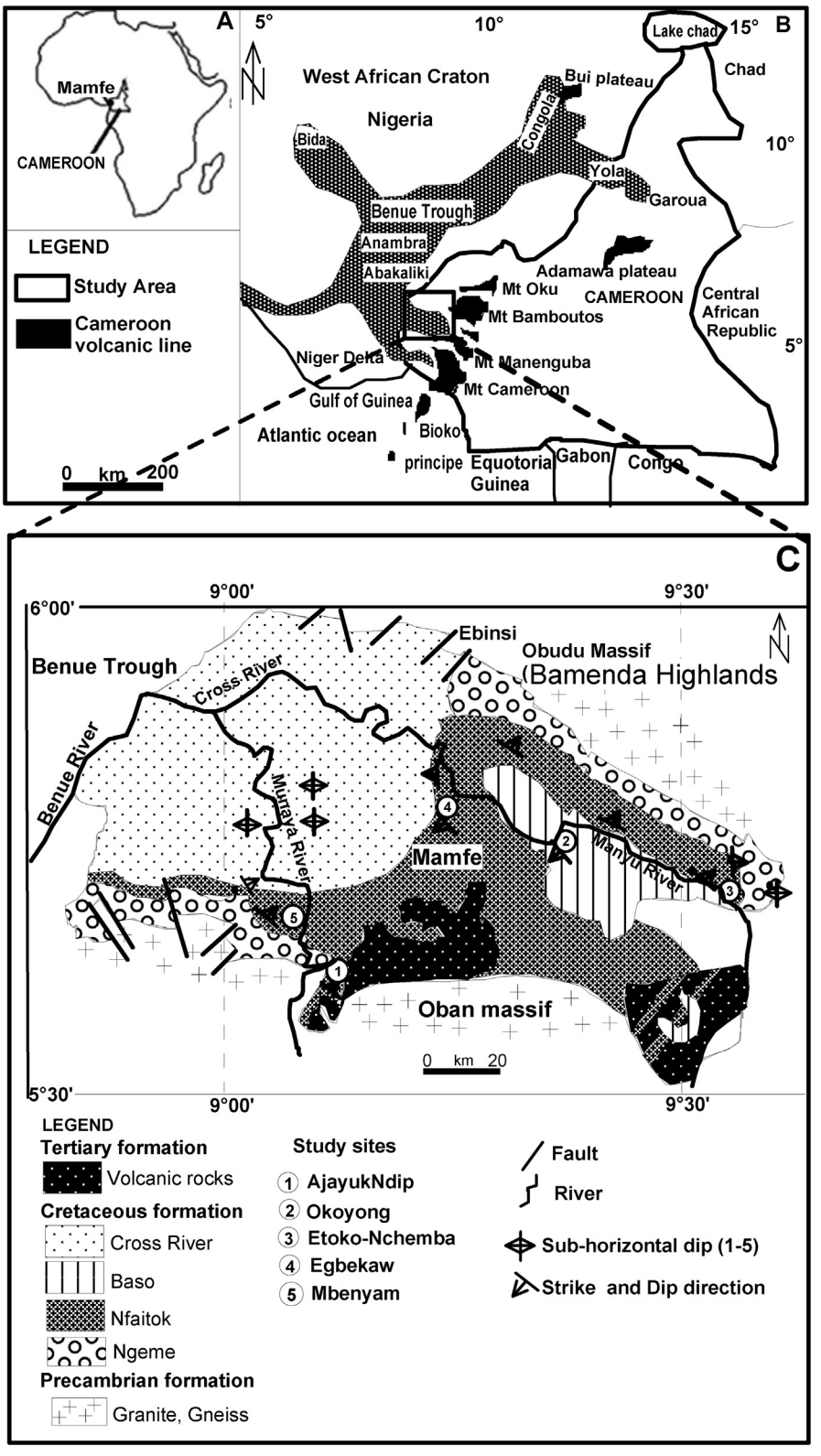

Fig. 1. Localization of the study site on the geologic map of the Mamfe basin (redrawn from Eyong et al., 2013).

https://doi.org/10.1016/j.heliyon.2019.e01140

The magmatic and metamorphic rocks formed the Precambrian basements and margin rocks of the basin overlain by a Cretaceous sedimentary cover representing the basin strata (Bokanda et al., 2018b). Both the Precambrian and Cretaceous cover are intruded by volcanic rocks of a basaltic, trachytic and doleritic composition. The sedimentary strata filling the basin include; conglomerates, sandstones, shales, and limestones (Eyong et al., 2013). The sandstones are locally fine to coarse-grained, friable to well-hardened cross-bedded pebbly to mostly massive, with variable colors ranging from white to brown, green, or pink with poorly sorted angular to sub-rounded grains (Eyong et al., 2013). Soft sediments deformation structures and clastic dykes are mostly associated with fine-grained sandstones and mudstones (Bokanda et al., 2018a).

3. Methods

Macroscopic and microscopic petrography was executed on the studied samples. Heavy mineral petrography was also effectuated. Microscopic observation in thin section was done at the laboratory of petrology and structural geology, University of Yaoundé I, Cameroon under the supervision of Dr. Milan S. Tchouatcha. Mineral identification and volume (Modal) semi-quantitative proportion of minerals species were done following the methods used in Ahmer and Muhammad, 2017.

The heavy mineral analysis was carried following the methods of Tchouatcha et al. (2016). Samples were crushed to sand particles sizes (100−200 microns). The crush samples are then decalcified with dilute hydrochloric acid (HCl). The decalcified dried samples are then separated by a heavy Bromoform liquid ($d = 2.89$) in other to extract the heavy minerals ($d > 2.89$).

A Geochemical analysis was performed on sandstones representing the five studied sites. The samples were carefully selected and crushed at the Institute of geological mining and research, Nkolbison Cameroon. The analytical procedures were performed at the laboratory of geology, Lakehead University using the ICP-AES Method. The protocols can be seen in Bokanda et al. (2018b).

4. Results

4.1. Petrography analysis

Sandstones are generally coarse to very coarse grained with heterogranular textures in hand observation. The conglomerates enclose clasts of gneiss, quartzites, and mica schist. The friable samples comprise of angular clastic materials whereas sub-rounded clast with smooth edges is observed in lithified samples. The clastic materials display variable sizes ranging from granules (3 mm), pebble (5−11 mm) to cable (25−50 mm). Generally, both sandstones and conglomeratic sandstones

https://doi.org/10.1016/j.heliyon.2019.e01140

include quartz, feldspars, rock fragments, matrix and accessory minerals of variable proportions (Table 1) (Fig. 2a). Quartz is the most prevailing mineral ranging from 55 to 65%, averaging 60 % of the overall composition. Quartz exists as monocrystalline, and polycrystalline (Fig. 2b). The monocrystalline quartz grains make up a range of 69−89, averaging 79 %, and polycrystalline quartz grains sum up on average 22 %. Orthoclase, microcline, and albite are the most dominant feldspars. The proportion of feldspars ranges from 25 to 33 %, averaging 29 %. Rock fragments constitute an average of 11%. Biotite and muscovite occur in these samples with

Table 1. Recalculated Modal point count. Qm(nu)= Non undulatary monocrystalline quartz, Qm(u) = Undulatary monocrystalline quartz, Qt= total quartz, (P+M)= plagioclase feldspars plus microcline, Ft = total feldspars, Rft= total rock fragments.

Samples	Qp (<3)	Qm (nu)	Qm(u)	Qt	Ft (P+M)	Rft	Total (%)	Qt/Rft+Ft	Qp/Rft+Ft
Site 1									
BS1	13	22	25	60	25	15	100	1.50	0.33
BS2	10	26	29	65	26	9	100	1.86	0.29
BS3	12	27	23	62	28	10	100	1.63	0.21
BS4	10	21	29	60	29	11	100	1.50	0.25
BS5	9	26	24	59	30	11	100	1.44	0.22
BS6	6	23	26	55	33	12	100	1.22	0.13
Site 2									
BS7	8	27	23	58	30	12	100	1.41	0.20
BS8	9	22	29	60	28	12	100	1.50	0.23
BS9	10	23	27	60	28	12	100	1.50	0.25
BS10	9	27	28	62	29	9	100	1.63	0.22
BS11	13	26	22	61	32	7	100	1.56	0.33
Site 3									
BS12	8	30	25	63	25	12	100	1.70	0.22
BS13	12	28	22	62	28	10	100	1.63	0.21
BS14	6	25	24	55	33	12	100	1.22	0.13
BS15	23	23	27	62	28	10	100	1.63	0.22
BS16	8	20	35	63	26	11	100	1.70	0.22
BS17	13	24	23	60	26	14	100	1.50	0.33
Site 4									
BS18	10	28	25	63	26	11	100	1.70	0.27
BS19	23	23	27	62	28	10	100	1.63	0.21
BS20	9	28	25	61	28	11	100	1.56	0.23
BS21	10	25	23	58	29	13	100	1.38	0.24
BS22	7	27	23	57	27	16	100	1.33	0.16
Site 5									
MSG1	11	24	25	60	26	14	100	1.50	0.26
MSG2	9	24	26	59	26	15	100	1.44	0.21

https://doi.org/10.1016/j.heliyon.2019.e01140

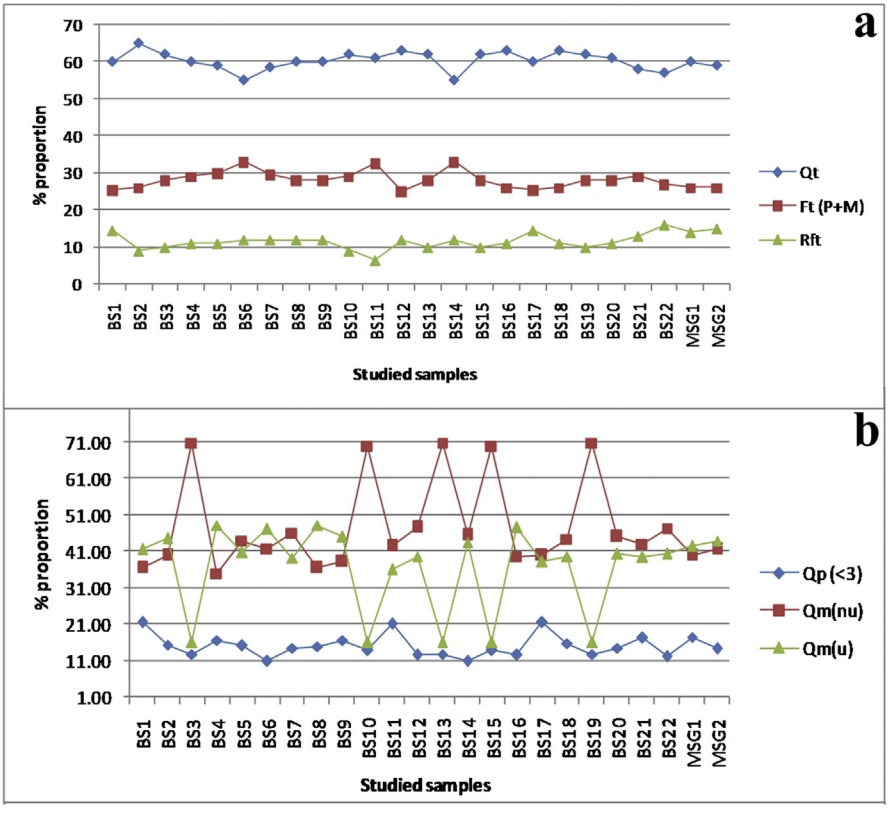

Fig. 2. Comparative modal proportion of sandstones and conglomeratic sandstones infer from (a,b) thin section petrography.

muscovite occurring frequently than biotite. These detrital framework grains are mostly bound together by calcite cement and matrix for carbonate sandstone, whereas clayey ferruginous cement and matrix are noted for noncarbonate sandstones.

4.2. Heavy mineral description

The heavy mineral suites present in the Mamfe sandstones are; zircon, tourmaline, kyanite, augite, garnets, hornblende, epidotes, diopside, muscovites, biotites, augite, apatite, sillimanite, zoisite and opaque minerals. These minerals vary in proportions in the different samples as seen in Fig. 3. The diagnostic features of the heavy mineral assemblages are summarized below.

Zircon: The grains are colorless to light pink, pyramidal and sub rounded to sub-angular constituting 9% of the heavy mineral assemblage. The grains are easily identifiable owing to their high relief and high order of interference color (Fig. 4a).

Kyanite: Kyanite occurs as pale green, elongated and sub-rounded to sub-angular shape. The percentage of kyanite is 8% (Fig. 4b).

https://doi.org/10.1016/j.heliyon.2019.e01140

Tourmaline: The grains are pleochroic, prismatic, pale-green to grayish in color and are about 2% of the total heavy minerals. Dominantly the grains are angular, fractured and contain inclusions (Fig. 4c).

Andalusite: Generally, andalusite grains exhibit a gray color with a light yellow spot at the center. The grains are sub-rounded and constitute 1% of the heavy mineral assemblage (Fig. 4d).

Biotite: It constitutes 3% of the heavy mineral assemblage. The flaky biotite grains are angular to sub angular and pale-yellow to reddish-brown in color (Fig. 4e).

Muscovite: The muscovites grains have a sub-angular to angular outline. It constitutes 3% of the heavy mineral assemblage. The cleavage flakes of muscovites exhibit pale green to pale brown color (Fig. 4f).

Diopside: Under reflected light, the sub-angular to sub-rounded diopside grains exhibit greenish color and are colorless under polarized light. It constitutes 2% of the total mineral assemblage (Fig. 4g1,2).

Epidote: It constitutes 5% of the heavies. The grains show pale green to a slightly grayish color. The grains are sub-rounded, fractured and some occur as an irregular shape (Fig. 4h).

Apatite: Apatite occurs as faint yellow to light brown in color, elongated and sub-rounded in shape. The percentage of apatite is 2% (Fig. 4i).

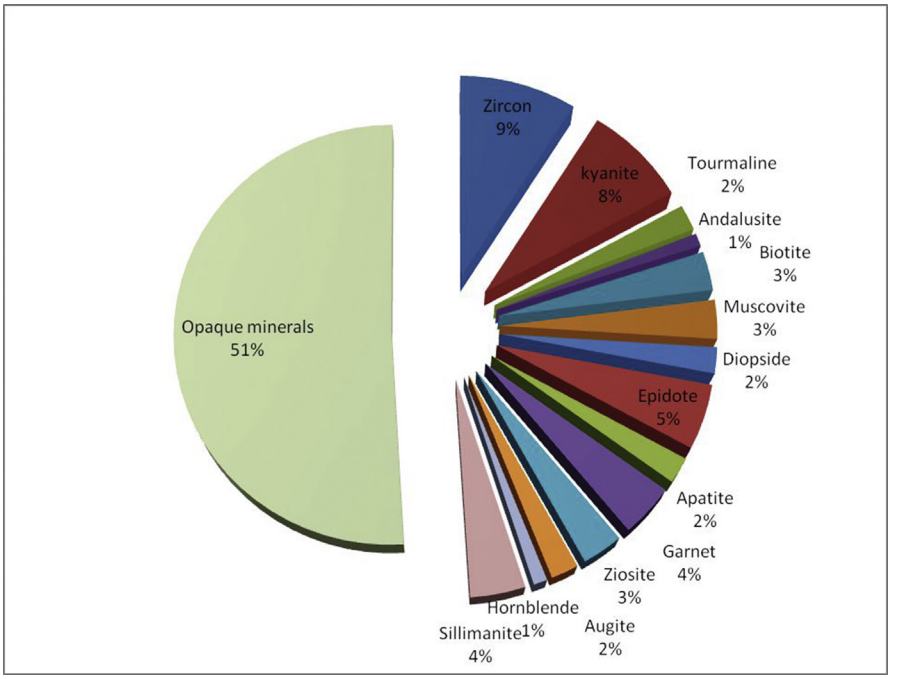

Fig. 3. Pie chart of heavy minerals proportions.

https://doi.org/10.1016/j.heliyon.2019.e01140

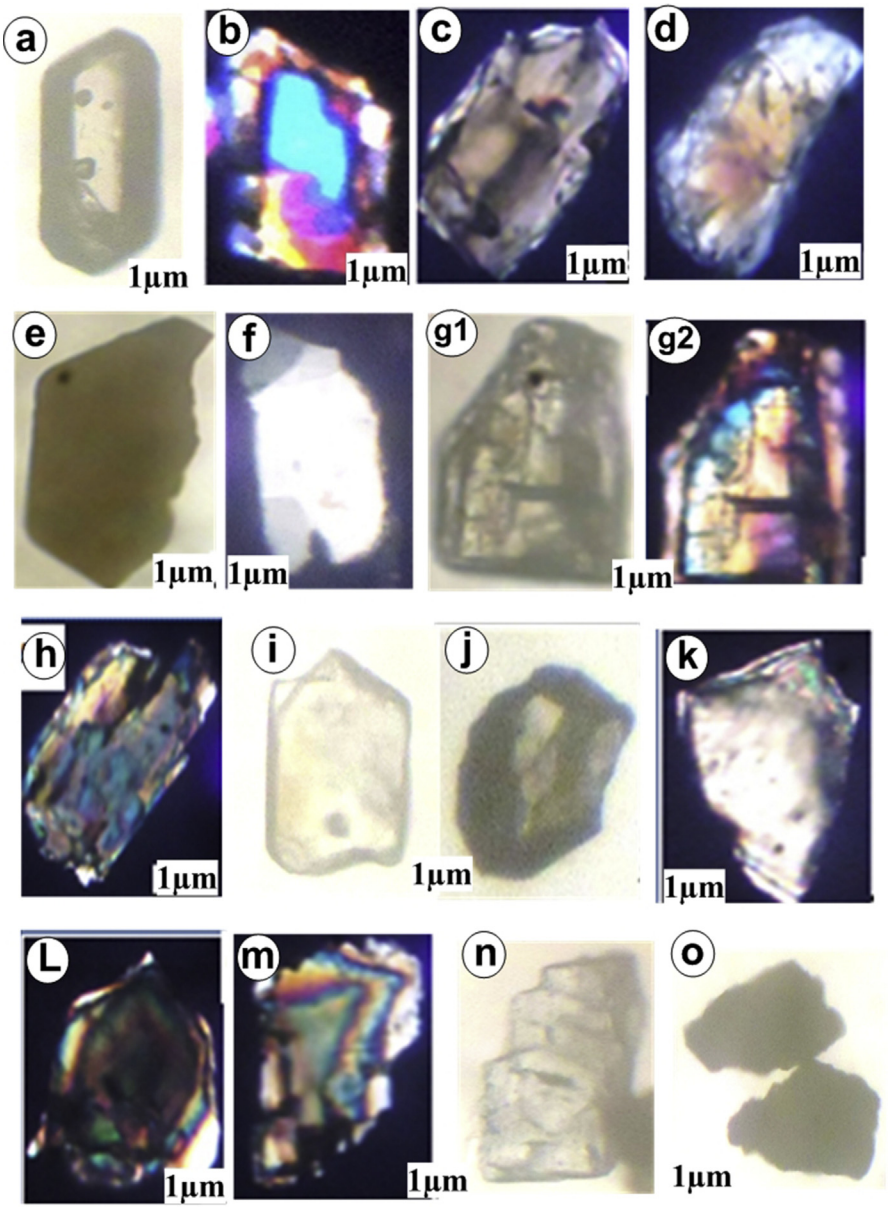

Fig. 4. Microphotograph of heavy minerals in the Mamfe sandstones and conglomeratic sandstones: (a) Zircon, (b) Kyanite, (c)Tourmaline, (d) Andalusite, (e) Biotite, (f) Muscovite (g1,2) Diopside, (h) Epidote, (i) Apatite, (j) Garnet, (k) Zoisite, (L) Augite, (m) Hornblende, (n) Sillimanite, (o) Opaque minerals.

Garnet: Garnet constitutes 4% of the heavy mineral assemblage. The grains are black in appearance and have a sub-angular to sub-rounded outline (Fig. 4j).

Zoisite: It constitutes 3% of the heavies. Zoisite grains exhibit various tints of pale green, colorless and occur as sub-angular to sub-rounded grains (Fig. 4k).

Augite: Augites are pale green, sub-angular and constitute 2% of total heavy mineral assemblage (Fig. 4l).

https://doi.org/10.1016/j.heliyon.2019.e01140

Hornblende: Hornblende is very rare with weak proportion (1%). Its displays pale green color and very angular-angular forms (Fig. 4m).

Sillimanite: They form euhedral crystals with a fibrous prismatic shape. Sillimanite is less abundant; it is angular and very slightly fibrous, and colorless. They have a fairly high relief and display parallel extinction angle. They constitutes 4 % of the heavy minerals assemblage (Fig. 4n).

Opaque mineral: These are oxides of iron, black in color and remain in extinction when the analyzer is in place. Many forms are noticeable, sub-angular, angular, and sometimes sub-rounded. Opaque mineral constitutes 51 % of the heavy minerals assemblage (Fig. 4o).

4.3. Diagenetic signatures

The key diagenetic processes that have affected the sandstones of the Mamfe basin are mechanical compaction and Authigenic processes.

4.3.1. Mechanical compaction

The sandstones of the Mamfe basin experienced moderate-intense physical and chemical compaction during their progressive burial. This is exposed by the alteration in grain contacts (concavo-convex) and sutured contacts (point contacts and long contact) of nearby grains (Fig. 5c, d, e, f, h). The overburden that compact the sediments also resulted in the fracturing of some of the grains, particularly the feldspar and muscovite (Fig. 5a, d). Some muscovite grains were completely deformed in shape. In a few cases, mica flakes are cracked or bent (Fig. 5a, d). Long contacts are common in the examined samples and their existence points to a moderate degree of compaction (Fig. 5e, h). Incessant burial resulted to increase compaction and porosity loss either by slippage or grain rotation, leading to final fracturing of resistant minerals. This causes pressure as the key processes for the dissolution of minerals from grain to grain contacts (boundaries) into an aqueous pore fluid in relatively high-stress areas. Occasionally, the deformed grains of quartz and muscovite are as a result of pressure dissolution.

4.3.2. Authigenesis

The Mamfe basin sandstones have undergone cementation (Quartz overgrowth) and replacement (Fig. 5).

4.3.2.1. Cementation

The studied sandstones disclose three types of cement, which are quartz cement, calcite cement, and feldspar cement.

Precipitation of silica between grains interspaces results in quartz cementation. Quartz cement occurs both as overgrowths (Fig. 5c, f) and fine granular quartz filling

https://doi.org/10.1016/j.heliyon.2019.e01140

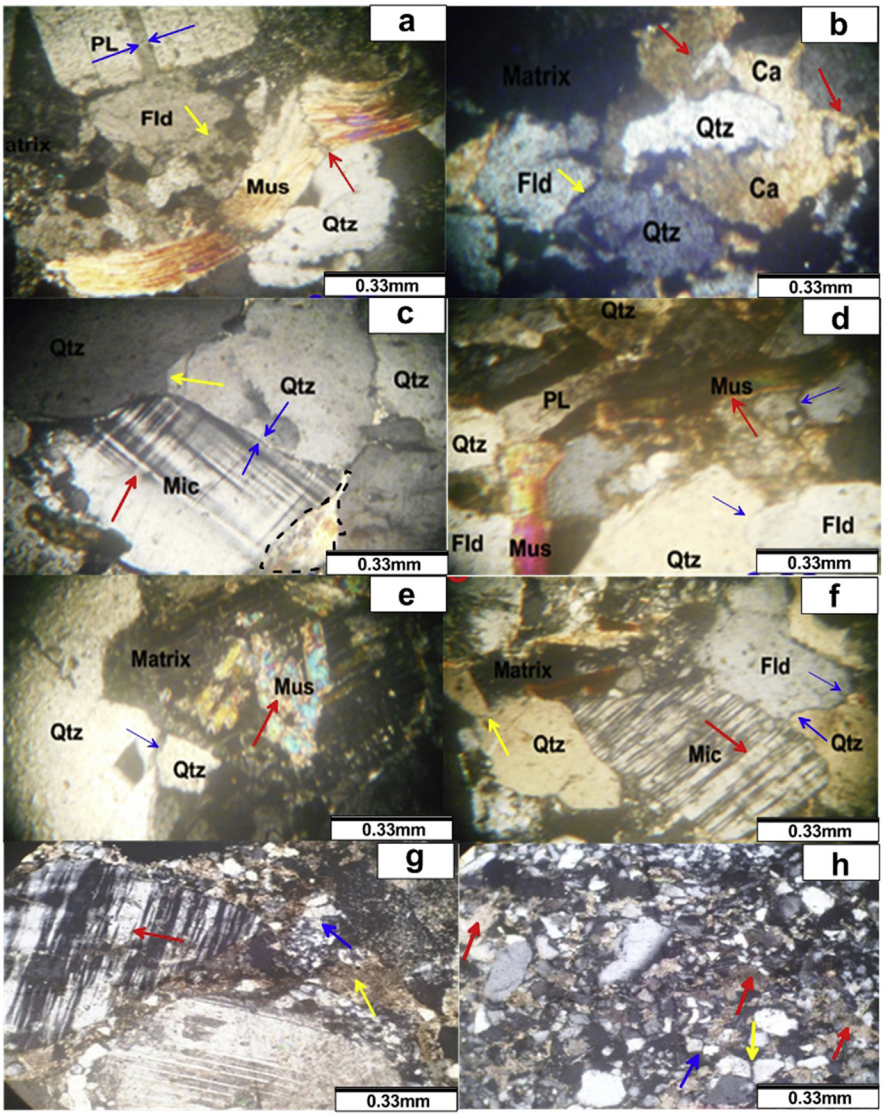

Fig. 5. Microphotographs of sandstones and conglomeratic sandstones: (a) Feldspar filling (blue arrow), feldspars overgrowth (yellow arrow) and muscovite deformation (red arrow) (b) Dissolution cracks (yellow arrow) and calcite replacement of quartz and feldspars (red arrow) (c) Grain to grain contact (blue arrow), quartz overgrowth (yellow arrow), Albitization (red arrow), clayey ferruginous matrix with feldspartic cements inbetween detrital grains (broken line) (d) Mica deformation (red arrow), concavo convex grain contact (blue arrow). (e) Chloritization or seritizsation (red arrow), long contact (blue arrow). (f) Albitization (red arrow), feldspars and quartz overgrowth creating a concavo convex contact (blue arrow), point contact (yellow arrow). (g) Albitization (red arrow), fine granular quartz cement (blue arrow), brownish red clay matrix (yellow arrow). (h) Long contact (yellow arrow), point contact (blue arrow) and calcite matrix (red arrow).

(Fig. 5c, g) pore spaces in the rocks. Outward growth of detrital quartz grain surface occurs as quartz overgrowth with some having optical characteristics as the original detrital quartz grains. Euhedral crystal faces occur as a result of overgrowths.

https://doi.org/10.1016/j.heliyon.2019.e01140

Calcite cementation is another type of cement in the Mamfe sandstone. It occurs mainly as a pore-filling and replacement mineral of clay matrix and detrital grains. Spaces between quartz and feldspars grains or their margins are partially or totally and sometimes locally occupy by calcite. Most of the clay minerals (matrix) and detrital grains were seriously attacked and replaced by calcite (Fig. 5b). Quartz overgrowths are replaced by calcite. Dissolution of feldspar creates pores which are mostly filled by calcite.

Minor cement type such as feldspar cement occurs as pore-filling feldspar and overgrowths (Fig. 5a). Feldspar overgrowths behave as authigenic feldspar pore-filling cement. Most of feldspar syntaxial overgrowths are associated with quartz overgrowths (Fig. 5a, c, f).

4.3.2.2. Mineral replacement

The Mamfe sandstones display mineral replacements such as quartz, clay matrix and feldspar replaced by calcite and microcline replaced by albite (albitization).

Calcite replaced both the clay matrix and framework grains (Fig. 5b), i.e., the detrital feldspars, quartz, and rock fragments are replaced by calcite. The feldspars affected are the microcline and sometimes plagioclase. Calcites replacement of the feldspars also leads to the creation of pores spaces in sediments.

Albite completely or partially replaced microcline and anorthite (Ca-feldspar) grains. In the case of the Mamfe sandstones, albitization of K-feldspars (microcline) is one of the major diagenetic changes during burial diagenesis. Albite replaced particularly the microcline mineral grains (Fig. 5c, f, g). Albite formed through replacement was revealed by the blocky to tabular sector extinction patterns where incomplete replacement occurred (Fig. 5c, f, g). Microfractures within framework grains, cleavages, and grain margin contact are mostly affected by Albitization.

5. Discussion

5.1. Source rock composition

Petrographic and heavy mineral analyses have been widely used by different authors (Blatt and Tracy, 1996; and Basu et al., 1975) in order to determine the nature of source rocks lithology and tectonic history of the source area during the time of deposition. The study of quartz, feldspars, lithic fragments, and other accessory minerals have provided evidence of the lithologic and tectonic sources to the study of sandstones.

According to Blatt and Tracy (1996) and Basu et al. (1975), quartz typology discloses different lithologic sources. Monocrystalline quartz grains present in these

https://doi.org/10.1016/j.heliyon.2019.e01140

sandstones are indicative of a granitic source (Ahmer and Muhammad, 2017). The presence of undulatory quartz notice in these sandstones suggests a metamorphic source whereas the few polycrystalline grains are evidence of derivation from gneissic and other highly metamorphic rocks.

The orthoclase and microcline observed in the studied sandstones are mostly derived from plutonic felsic rocks and high-grade metamorphic rocks such as granite and/gneiss, while the less abundant plagioclase feldspars are mainly common in low-grade metamorphic rocks (Boggs, 2006). Compositionally, the studied sandstones are composed of a high proportion of non-undulatory quartz and microcline. This satisfactory composition of the different quartz typology and feldspars suggest plutonic sources.

The lithic clasts, being a definite indicator of the provenance, disclose a mixed source comprising of felsic plutonic and metamorphic rocks. Micas present in these sandstones point toward a low-grade metamorphic rock like quartzite, schist, gneiss, and granite.

A plot on the diamond diagram of Basu et al. (1975) reveals middle to upper-rank metamorphic source rocks with only a few samples source from a plutonic origin (Fig. 6a). In general, the petrographic study advocates a mixture of felsic plutonic and metamorphic rocks provenance for these sandstones. The assertion of a mixed metamorphic and felsic magmatic provenance is supported by the fact that, most of the basins margins are composed of Precambrian gneissic and granitic rocks which are unconformable overly by the Cretaceous sedimentary formations which are together cross cut by volcanic rocks of Cenozoic age.

Heavy mineral suits as provenance indicators have been widely discussed by Srivastova et al. (2015) and Ralte (2012). Following the heavy mineral assemblage in relation to source rocks proposed by Sengupta (2017), it may be suggested that the Mamfe sandstones are derived from mixed metamorphic and acid plutonic magmatic rocks (Table 2).

The ratios among immobile trace elements such as Cr/Th, Th/Sc, Th/Co, and La/Sc are well thought-out to suitable markers of source rock provenance (Taylor and McLennan, 1985; Cullers and Podkovyrov, 2000). The ratios of these elements resulting from mafic, and felsic sediments as well as the upper continental crust were judge against those of the present study (Table 3). Armstrong-Altrin et al. (2004) denote that, the La/Sc and Th/Sc ratios of mafic sediments are always lower than sediments resulting from mafic rocks. Although slightly inferior values of Th/Sc ratios are revealed by some of the sandstones, however, the Th/Sc ratio of the present study falls within the ranges of felsic rocks and are still much superior to those of mafic rocks demonstrating a felsic source for the study sandstones. In addition, some studied sandstones disclose ratios of Cr/Th close to those of UCC (Cr/Th = 7.76,

https://doi.org/10.1016/j.heliyon.2019.e01140

Table 2. Heavy mineral assemblages of major source rocks (after Sengupta, S.M., 2017).

Heavy mineral assemblages	Source rocks
Apatite, biotite, hornblende, Monazite, Muscovite, pink tourmaline, Zircon	Acid igneouse rock
Fluorite, garnet, Muscovite, topaz, Monazite, blue tourmaline	Granite pegmatite
Augite, diopside, hyperstene, magnetite, olivine, chromite	Basic igneouse rocks
Andalusite, garnet, staurolite, zoisite, epidote, kyanite, sillimanite	Metamorphic rocks
Barite, iron ores, rutile, tourmaline, rounded grain zircon	Reworked sediments

Table 3. Significant provenance trace elements (ppm).

	Th	U	Co	Sc	Cr	Ni	La
Site 1	10.8	4.7	14.9	8	63.63	28	37
Site 2	9	5.3	3.4	4	96.48	15	50.2
Site 3	27.5	10.7	22.8	14	53.24	47	100
Site 4	8.6	2.4	8	9	50.58	10	48.7
Site 5	21.6	8.7	13.17	6	108.56	28	95.9

McLennan et al., 2006). The Th/Co ratios of the present study samples also fall in the neighborhood of felsic rocks and are exceptionally close to those of UCC (Tables 3 and 4). The Ni proportions of the present study sandstones are inferior to 100 ppm while the Cr proportions are inferior to 150 ppm indicating a source rock of felsic composition (Garver et al., 1996). The assessments show that the majority of our data are within the range of felsic source rocks.

5.2. Tectonic setting

In the QtFL diagrams (Dickinson, 1988) the studied sandstones falls within the transition domain of a continental block provenance field indicating their occurrences in an uplifted basement to sub-cratonic stable shelf settings (Fig. 6b, d). Basement uplifts bounded by faults discard arkosic sands into adjacent basins whereas craton interiors are shield domains of low lying granitic and gneissic coverage which produces sand on erosion. The sandstones are arkose which is a characteristic of residual or local deposits derived from granitic basement rocks (Fig. 6c). The mineralogical and textural immaturity of the sandstones coupled with abundant angular grains and feldspars supports sediments mostly derive from first cycle origin. The presence of unaltered feldspars enclose in these samples hold up the idea of origin from a moderate to high relief source couple with rapid erosion and deposition in nearby basins with trivial reworking.

https://doi.org/10.1016/j.heliyon.2019.e01140

Table 4. Trace element calculated ratios of the studied sites sandstones.

	Mamfe sandstones[1]					Range of sediments[2]		UCC[3]
	Site 1	Site 2	Site 3	Site 4	Site 5	Felsic	Mafic	
Th/Cr	0.16	0.093	0.51	0.17	0.19	0.13−2.7	0.018−0.046	0.13
La/Sc	4.63	12.55	7.17	5.14	15.98	2.51−16.3	0.43−0.86	2.21
Th/Sc	1.35	2.25	1.96	0.96	3.06	0.84−20.5	0.05−0.22	0.97
Th/Co	0.72	2.65	1.21	1.08	1.58	0.67−19.4	0.04−1.4	0.63
Cr/Th	5.89	10.72	1.93	5.88	5.02	4.0−15.0	25−500	7.76

[1]This study, [2](Cullers and Podkovyrov, 2000, 2002; [3]Taylor and McLennan, 1985).

5.3. Paleoclimate and depositional environment

Paleoclimate studies facilitate the understanding of weathering processes in the source area as well as the climatic condition of deposition. Climatic signatures are preserved in sands during deposition provided they do not suffer sedimentary differentiation followed by long-distance transport and deposition in rough water littoral environment. Sandstones compositions are not only affected by tectonics, transportation history but also by sedimentary processes within the depositional basin and palaeoclimate (Suttner and Dutta, 1986). The bivariant log/log plot study based on the ratios of Qp/(F+R) and (Qm+Qp)/(F+R) is one of the most useful bases for discriminating climaticconditions (Suttner and Dutta, 1986). From the bivariant log-log plot of the above ratios (Fig. 6e), it can be inferred that the studied samples were deposited under a semi-humid climatic condition (see Fig. 6e).

The quartz grains incorporated in the sandstones and conglomeratic sandstones reveals abundant of very angular to angular shining grains (Not Worn) particles of approximately 95−99% and an average of 97 %. Sub-angular to sub-rounded shining (SASRS) particles were less abundant with an estimated range of 1−7%, averaging 4%. The Not Worn grains result from sediment transport in an aqueous environment over a moderate or short distance (Pettijohn, 1975). The sources of these particles are proximal to sub-proximal, indicating that they are not far from their source. It also gives information on that the transportation was fluvial proving that; there was a lot of vegetation at the time of their transportation which prevents the action of wind. According to Cailleux (1946) and Cailleux and Tricart, 1959, the SASRS grains are the result of moderate-distance transport in continental aquatic environments such as rivers or streams which causes their edges to be less rounded and shinning. The characteristics of the quartz grains in this study also indicate transport through an aqueous environment. All these sediments were transported by rivers.

5.4. Diagenesis

Diagenesis occurs uniquely in consolidated sedimentary rocks. Diagenesis infers from petrographic studies have widely been discussed by some authors

https://doi.org/10.1016/j.heliyon.2019.e01140

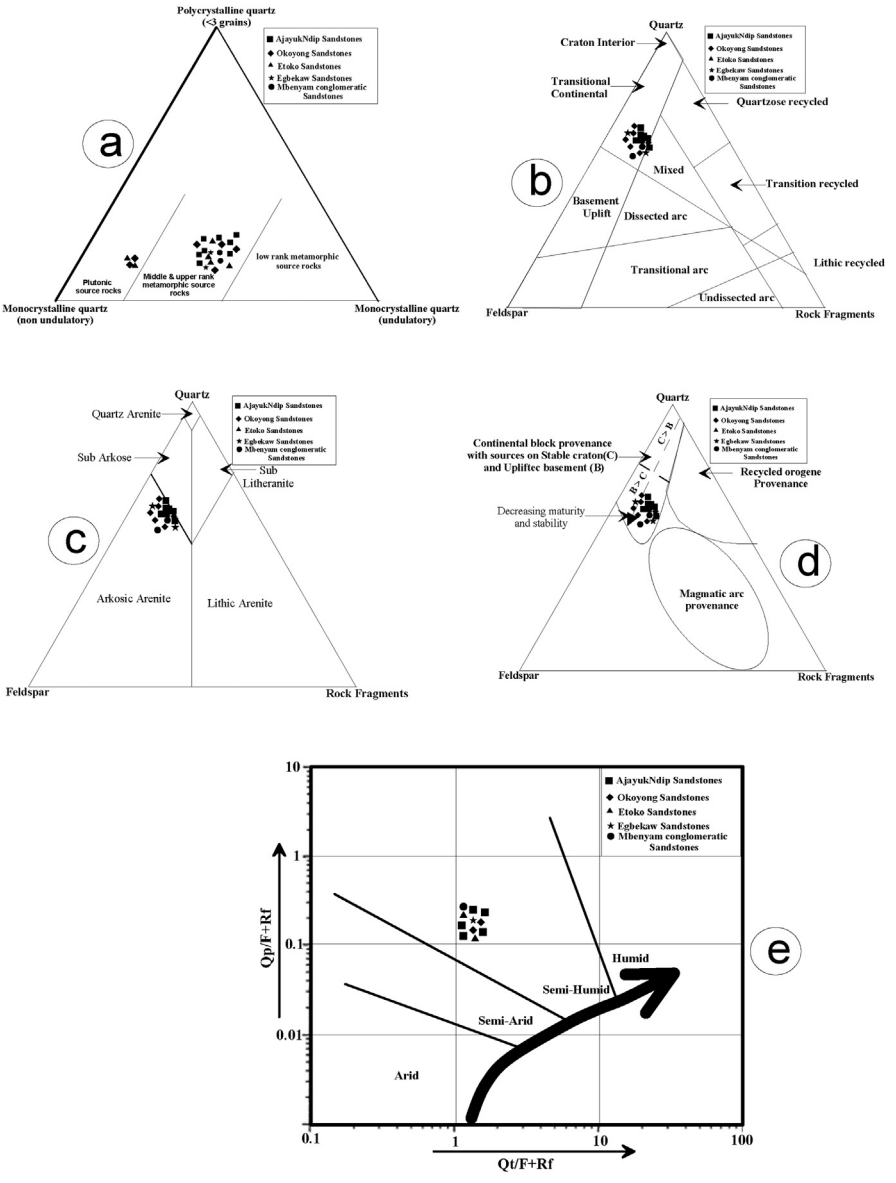

Fig. 6. Discriminate diagrams of the Mamfe sandstones: (a) Diamond diagram (Basu et al., 1975) to determine the provenance, (b, and d) QtFL ternary plot after Dickinson (1985) for the determination of the tectonic setting of the provenance, (c) QFL-triangular plot for the classification of sandstones (Ahmer and Muhammad, 2017), (e) Paleoclimate discrimination plot for the Mamfe sandstones (Suttner and Dutta, 1986).

(Srivastava et al., 2015; Christopher et al., 2017) with different points of views. Christopher et al. (2017) studied the Ecca Group Sandstones in the Eastern Cape Province, South Africa and proposed a three (3) stage diagenesis (early, burial and uplift) affecting the sandstones. According to Christopher et al. (2017), the early stage of diagenesis is characterized by matrix and cement precipitation, authigenic mineral formation, compaction, and minor cementation; burial stage characterized

https://doi.org/10.1016/j.heliyon.2019.e01140

by physical and chemical compaction, mineral replacement, grain deformation, and cementation, while uplift is mostly represented by secondary porosity and iron oxides reddish to brownish stains. Studies carried on the Nagaland sandstones in India by Srivastava et al. (2015) postulated three stages of diagenesis namely; redoxmorphic, locomorphic and phyllomorphic. Features characterizing these stages are; precipitation of iron oxide for the redoxomorphic stage (Bjorkum and Gjelvik, 1988), silica over growth and modified grain to grain contacts, corrosion of detrital grains and alteration of feldspar for the locomorphic stage (Srivastava et al., 2015) and, flaky minerals reconstitution for phyllomorphic stage.

Texturally the Mamfe sandstones are friable to lithified, reddish to brownish in color for some and grayish white mostly for some conglomeratic sandstone. Compositionally, some of these rocks contain ferruginous, feldspars and quartz matrix, with an indication of processes like replacement of minerals, cementations, grained deformation and fracturing. Following the concomitant petrographic characteristics of the Mamfe sandstones and those studied by Srivastava et al. (2015) and Christopher et al. (2017), one can by no doubt conclude that the Mamfe sandstones have been affected by early, burial and uplift diagenetic processes during their redoxmorphic, locomorphic and phyllomorphic diagenetic stages.

6. Conclusion

The following conclusions can be drawn from the study of the Mamfe sandstones:

(1) Modal analysis data from petrography and heavy minerals indicate that the detritus was derived from felsic igneous (granite) and metamorphic (gneiss, schist, quartzite) rocks.

(2) Trace element geochemical data indicates that the detritus was derived from felsic sources. This source rocks points to the Precambrian granite and gneissic rocks which form the basement and margin of the basin.

(3) Major framework mineral components of the sandstones point out that the sediments derived their detritus from a transitional continental region of continental block provenance. It also discloses a redoxmorphic, locomorphic and phyllomorphic diagenetic stages with evidence of early, burial and uplift diagenetic process.

(4) The high proportion of angular feldspars grains reveal a high relief and rapid erosion leading to the formation of mineralogically and texturally immature sandstones which have been classified as arkose deposited in a fluvial environment.

(6) Abundant not worn angular to sub-angular shining grains of quartz reveals a fluvial depositional environment under semi-humid climate.

https://doi.org/10.1016/j.heliyon.2019.e01140

Declarations

Author contribution statement

Eric Bokanda Ekoko, Emile Ekomane, Nguemo Gatien Romuald Kenfack, Isaac Konfor Njilah, Ethel Nkongho Ashukem, Paul Tematio, Salomon Betrant Bisse, Gabriel Ngueutchoua, Shelly Ngui Orock, Cedric Belinga Belinga: Conceived and designed the experiments; Performed the experiments; Analyzed and interpreted the data; Contributed reagents, materials, analysis tools or data; Wrote the paper.

Funding statement

This research did not receive any specific grant from funding agencies in the public, commercial, or not-for-profit sectors.

Competing interest statement

The authors declare no conflict of interest.

Additional information

No additional information is available for this paper.

Acknowledgements

The authors will want to thank Dr. Eyong John Takam for the field work assistance, Dr. Milan S. Tchouatcha, for the assistance in the Petrogaphic review of thin sections and heavy minerals analysis. Thanks to the anonymous reviewers whose remarks improved this article.

References

Ahmer, B., Muhammad, S.K., 2017. Petrography and provenance of sandstone and studies of shale of Kuldana formation, Kalamula and Khursheedabad area, Kahuta. Azad Kashmir Earth Sci. Malaysia (ESMY) 1 (1), 21−31.

Armstrong-Altrin, J.S., Lee, Y.I., Verma, S.P., Ramasamy, S., 2004. Geochemistry of sandstones from the upper Miocene Kudankulam Formation, southern India: implications for provenance, weathering, and tectonic setting. J. Sediment. Res. 74 (2), 285−297.

Basu, A., Young, S.W., Suttner, L.J., James, W.C., Mack, G.H., 1975. Re-evaluation of the use of undulatory extinction and polycrystallinity in detrital quartz for provenance interpretation. J. Sediment. Petrol. 45, 871−882.

https://doi.org/10.1016/j.heliyon.2019.e01140

Bjorkum, Gjelvik, 1988. An isochemical model for formation of authegenic kaolinite, k-feldspar and illite in sediments. J. Sediment. Petrol. 58, 506–511.

Blatt, H., Tracy, R., 1996. Petrology, Igneous, Sedimentary and Metamorphic, second ed. W. H. Freeman Pub., New York. 497 pp.

Boggs, S.J., 2006. Principles of Sedimentology and Stratigraphy, fourth ed. Merril Publishing Company, Toronto.

Bokanda, E.E., Ekomane, E., Eyong, J.T., Njilah, I.K., Ashukem, E.N., Bisong, R.N., Bisse, S.B., 2018a. Genesis of clastic dykes and soft sediment deformation structures in the Mamfe basin, South-West region, Cameroon: field geology approach. J. Geol. Res. 8.

Bokanda, E.E., Ekomane, E., Fralick, P., Njilah, I.K., Bisse, S.B., Akono, D.F., Ekoa, B.A.Z., 2018b. Geochemical characteristics of shales in the Mamfe Basin, South West Cameroon: implication for depositional environments and oxidation conditions. J. Afr. Earth Sci. 149 (2019), 131–142.

Cailleux, L., 1946. Distinction des sables marins et fluviatiles. Bulletin de la Société Géologique de France, pp. 125–138.

Cailleux, A., Tricart, J., 1959. Initiation à l'étude des sables et des galets. Centre de documentation universitaire, fascicules, Paris, p. 202.

Christopher, B., Kuiwu, L., Oswald, G., 2017. Diagenesis and reservoir properties of the permian Ecca Group sandstones and mudrocks in the Eastern Cape Province, South Africa. Minerals 7, 88.

Critelli, S., 2018. Provenance of Mesozoic to Cenozoic circum-Mediterranean sandstones in relation to tectonic setting. Earth Sci. Rev. 185, 624–648.

Cullers, R.L., Podkovyrov, V.M., 2000. Geochemistry of the Mesoproterozoic Lakhanda shales in southeastern Yakutia, Russia: implications for mineralogical and provenance, and recycling. Precambrian Res. 104, 77–93.

Cullers, R.L., Podkovyrov, V.M., 2002. The source and origin of terrigenous sedimentary rocks in the Mesoproterozoic Uigroup, south-eastern Russia. Precambrian Res. 117, 157–183.

Dickinson, W.R., 1985. Interpreting provenance relations from detrital modes of sandstones. In: Zuffa, G.G. (Ed.), Provenance of Arenites. Reidel, Dordrecht, Holland, pp. 333–361.

Dickinson, W.R., 1988. Provenance and sediments dispersal in relation to palaeotectonics and palaeogeography of sedimentary basins. In: Kleinspehn, K.L., Paola, C. (Eds.), New Perspective in basin Analysis. Springer-Verlag, New York, pp. 3–25.

 https://doi.org/10.1016/j.heliyon.2019.e01140

Eyong, J.T., Wignall, P., Fontong, W.Y., Best, J., Hell, J.V., 2013. Paragenetic sequences of carbonate and sulphide minerals of the Mamfe Basin (Cameroon): indicators of palaeo-fluids, palaeo-oxygen levels and diagenetic zones. J. Afr. Earth Sci. 86, 25–44.

Garver, J.I., Royce, P.R., Smick, T.A., 1996. Chromium and nickel in shale of the Taconic Foreland; a case study for the provenance of fine-grained sediments with an ultramafic source. J. Sediment. Res. 66, 100–106.

Kanouo, N.S., Ekomane, E., Fouateu Yongue, R.S., Njonfang, E., Zaw, K., Changqian, David, R.L., Venkatesh, A.S., 2012. U–Pb ages for zircon grains from Nsanaragati Alluvial Gem placers: its correlation to the source rocks. Resour. Geol. 65 (2), 103–121.

Kanouo, N.S., Ekomane, E., Fouateu Yongue, R.S., Njonfang, E., Zaw, K., Changqian, Ghogomu, T.R., David, R.L., Venkatesh, A.S., 2015. Trace elements in corundum, chrysoberyl, and zircon: application to mineral exploration and provenance study of the western Mamfe gem clastic deposits (SW Cameroon, Central Africa). JAES 113, 35–50.

McLennan, S.M., Taylor, S.R., Hemming, S.R., 2006. Composition, differentiation, and evolution of continental crust: constraints from sedimentary rocks and heat flow. In: Brown, M., Rushmer, T. (Eds.), Evolution and Differentiation of the Continental Crust. Cambridge Univ. Press, pp. 92–134.

Pettijohn, F.J., 1975. Sedimentary rocks, third ed. Harper and Row Publish., New York, p. 628.

Ralte, V.Z., 2012. Heavy mineral analysis of Tipam sandstone near Buhchang village, Kolasib district, Mizoram, India. Sci. Vis. 12 (1), 22–31.

Sengupta, S.M., 2017. Introduction to Sedimentology, first ed. Routledge. 322 p.

Srivastava, Sk., Khrovu, V., Moalang, A.k., 2015. Petrography and diagenesis of palaeogene sandstones, south of Kohima Town, Nagaland, India. Int. J. Earth Sci. Eng. 08 (05), 2025–2032. October, 2015, ISSN: 0974-5904.

Suttner, L.J., Dutta, P.K., 1986. Alluvial sandstones and paleoclimate framework mineralogy. J. Sediment. Res. 56, 329–345.

Taylor, S.R., McLennan, S., 1985. The Continental Crust: its Composition and Evolution. Blackwell, Oxford, 312 p.

Tchouatcha, S.M., Njoya, A., Ganno, S., Toyama, R., Ngouem, P.A., Ngaha, P.R., 2016. Origin and paleoenvironment of pleistocene-holocene travertine deposit from the mbéré sedimentary sub-basin along the Central Cameroon shear zone: insights from petrology and palynology and evidence for neotectonics. JAES 118, 24–34p.

https://doi.org/10.1016/j.heliyon.2019.e01140